

Breaking of Emulsions with Chemical Additives: Using Surrogate Fluids to Develop a Novel Theoretical Framework and Its Application to Water-in-Crude Oil Emulsions

Huy-Hong-Quan Dinh,* Enric Santanach-Carreras, Véronique Schmitt, François Lequeux, and Pascal Panizza*



Cite This: *ACS Omega* 2021, 6, 27976–27983



Read Online

ACCESS |



Metrics & More

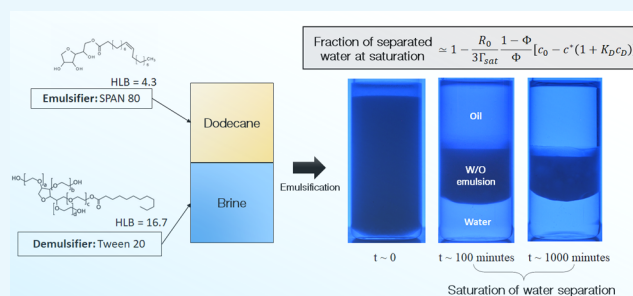


Article Recommendations



Supporting Information

ABSTRACT: We investigate the role of adding a water-soluble surfactant (Tween 20) that acts as a demulsifier on the stability of water-in-dodecane emulsions stabilized with Span 80. Performing bottle test experiments, we monitor the emulsion separation process. Initially, water droplets sediment fast (~ 10 min) until they become closely packed and form the so-called dense packed layer (DPL). The presence of the DPL, a long-lived metastable high-water-fraction (70–90%) emulsion separating bulk oil and water layers, slows down significantly the kinetics ($\sim 10^5$ min) of water separation. Once the DPL is formed, the ratio of the volume of separated water to the total water amount is called as water separation efficiency. We assume that the emulsion stability is reached when the coverage of the emulsifier surfactant exceeds 80% and use the ideal solution approximation. From that, we rationalize the water separation efficiency and the minimum demulsifier concentration required to maximize it, in terms of the mean droplet size, the surfactant concentrations, the total water volume fraction, and the adsorption strength of the water-soluble surfactant. Model predictions and experimental findings are in excellent agreement. We further test the validity and robustness of our theoretical model, by applying it successfully to data found in the literature on water-in-crude oil emulsion systems. Ultimately, our results prove that the efficiency of a demulsifier agent to break a W/O emulsion strongly correlates to its adsorption strength at the W/O interface, providing a novel contribution to the selection guidelines of chemical demulsifiers.



INTRODUCTION

Destabilization of water-in crude oil emulsions that form during oil extraction operations¹ is a key issue for the petroleum industry as their existence is highly detrimental both from a product quality point of view and from the additional charges they add to the costs of petroleum transport in pipelines and refining operations.² Water-in-crude oil emulsions *per se* are generally very stable because of the presence of surface-active endogenous species such as asphaltenes or resins.^{3,4} Under gravity settling, these metastable systems may last from a few months up to several years. To shorten their lifetime and accelerate the kinetics of phase separation, an effective method consists of adding some chemical agents to them to strongly enhance droplet coalescence. A simple and inexpensive method to evaluate the efficiency of such chemical agents is to perform bottle tests in which the lifetimes of bottle samples of emulsions, left at rest under gravity settling, are studied. Efficient demulsifier molecules for destabilizing W/O emulsions made of crude oil usually exhibit high values of hydrophilic–lipophilic balance (HLB)⁵ and number of ethylene oxide units per molecule (EON).⁶ In contrast to the endogenous species naturally found

in crude oil systems, such surfactant molecules are known to promote the formation of O/W emulsions. As a result of the co-adsorption of these respective molecules, the spontaneous curvature of the water–oil interface may evolve and lead to the possible destabilization of the W/O emulsion through coalescence events. Many experiments conducted by several research groups reveal that the efficiency of demulsifier additives for destabilizing water-in-crude oil emulsions strongly correlates with their adsorption strengths at the water–oil interface.^{7–12} However, the physical chemistry knowledge on the role of these chemical additives in the separation efficiency remains so far qualitative and empirical, and the physics behind this phenomenon is still poorly understood.

Received: July 20, 2021

Accepted: September 24, 2021

Published: October 13, 2021



In wash tanks as well as in bottle tests, water droplets sediment as a result of gravity mismatch between oil and water until they become closely packed and form the so-called dense packed layer (DPL), a high-water-fraction emulsion layer separating the oil and water volumes that have already demixed. In the DPL,^{13–15} the kinetics of phase separation considerably slows down as drainage requires oil to flow through the narrow interstitial channels separating water droplets. Furthermore, Dinh et al.¹⁵ have recently shown that emulsion droplets within the DPL are almost fully covered by surfactant molecules so that coalescence is also hindered.¹⁶ For these two reasons, DPLs are long-lived metastable emulsions. Once the DPL is formed, the volume fraction of separated water reaches a saturated value that we call water separation efficiency. In the oil industry, an essential task is therefore to find ways to maximize the water separation efficiency by adding, for instance, some demulsifier additives to the system. Despite a wealth of information on the topic, a comprehensive understanding of the phenomenon is still lacking and the choice of a demulsifier to reach an optimal formulation to destabilize the DPL remains so far qualitative and empirical.

In this study, by conducting bottle tests experiments on a model W/O emulsion system, we quantitatively investigate the effect of Tween 20, a water-soluble surfactant, on the occurrence of the DPL and on the water separation efficiency. By extending the theoretical framework introduced by Dinh et al.,¹⁵ we rationalize the strong correlation found between the efficiency of the demulsifier and its adsorption strength at the water–oil interface. We establish a simple analytical relationship between the water separation efficiency and the relevant physical and physicochemical parameters of the system, namely, the mean droplet size, the adsorption coefficient of the demulsifiers molecules at the water–oil interface, the oil–water volume ratio, and the concentrations of both emulsifier and demulsifier surfactants. Our findings show that the principal action of “good” demulsifiers at destabilizing emulsions is to reduce the volume of the dense emulsion zone, as a result of its strong adsorption on the surface of W/O droplets.

EFFECT OF ADDITIVE ON SURFACTANT-STABILIZED EMULSIONS SEPARATION: EXPERIMENTAL RESULTS AND DISCUSSION

While investigating the separation kinetics of emulsions (stabilized by large amounts of surfactant) occurring in bottle tests, we have noticed that all emulsions first undergo a gravity settling regime, where the droplets coalesce and fastly sediment before they form a so-called dense packed layer (DPL), a high-water-volume-fraction emulsion layer separating oil and water demixed phases (Figure 1). In the DPL, the droplet volume fraction is typically in the range [0.7–0.9] so that the kinetics of phase separation resulting from oil drainage considerably slows down. As a result, once formed, the DPL remains very stable and the water separation ratio therefore reaches an almost steady-state value, denoted \mathcal{W}_S . Thus, \mathcal{W}_S can be seen as the water separation efficiency of the emulsion system. Indeed, in the first witnessed regime, preceding the formation of the DPL, the droplet surfaces are not saturated with surfactant molecules so that coalescence easily occurs when two droplets collide.¹⁵ As the mean size of the emulsion droplets increases, the total surface of the water droplets

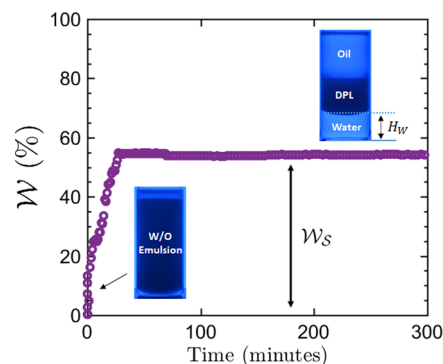


Figure 1. Variation of the water separation ratio as a function of rest time after emulsification observed in a bottle test. The W/O emulsion is stabilized by 800 ppm of Span 80 added to the oil (dodecane) phase. Its water volume fraction is $\Phi = 0.5$. The mean diameter of the droplets after emulsification is 20 μm .

decreases so that a higher surface concentration of surfactant molecules is achieved. When this surface concentration reaches Γ^* , a value that is roughly 80% of its saturation value, Γ_{sat} , coalescence between droplets becomes hindered and the long-lived metastable DPL forms. In line with this scenario, by writing the mass conservation of surfactant molecules between bulk and the W/O interface, one can derive a simple analytical expression of \mathcal{W}_S ,¹⁵ as shown below

$$\mathcal{W}_S = 1 - \frac{R_0}{3\Gamma^*} \frac{1 - \Phi}{\Phi} (c_0 - c^*) \quad (1)$$

where R_0 is the mean droplet size found at the beginning of the DPL regime, respectively; c_0 and c^* , respectively, stand for the emulsifier surfactant concentration and the minimum surfactant concentration value required to generate the DPL; Φ is the water volume fraction; and $\Gamma^* = 0.8\Gamma_{\text{sat}}$ with Γ_{sat} being the saturated excess surface concentration of the surfactant. In our model emulsion system (with no Tween 20), c^* is typically of the order of 20 ppm. We interestingly notice from the previous relationship (eq 1) that the thickness of the DPL increases with c_0 , the concentration of Span 80. Practically, this relationship allows one to predict the maximum amount of water that can be retrieved after the first separation regime that precedes the formation of the DPL and which typically lasts for a few hours. Very interestingly, our simple model yields a counterintuitive but interesting result: the smaller the droplet size, the larger the water separation ratio.

In an effort to understand and quantify the role of demulsifier on the stability of emulsions, we now perform similar bottle test experiments on the aforementioned W/O emulsion model system but to which we add varying amounts of Tween 20. The concentration of Tween 20 in the water phase is next denoted by c_D . Figure 2 displays images of bottle tests taken at the initial stage of the DPL for emulsions that only differ from the amounts of Tween 20 that is added into their respective water phases. This figure shows that the larger the concentrations of Tween 20, the larger the volume of demixed water when the DPL forms. This observation is qualitatively well explained if one recalls that because of its high HLB value (16.7), Tween 20 is a surfactant that has a natural tendency to form O/W emulsions. Consequently, when Tween 20 molecules adsorb on the W/O interface, which is stabilized by Span 80 molecules, they modify the spontaneous

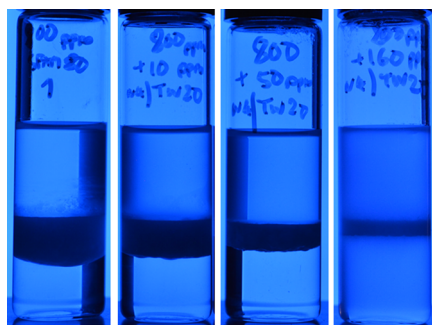


Figure 2. Photographs of bottle tests, 100 min after emulsification for various amounts of Tween 20 added to the same emulsion system. The oil phase is dodecane containing 800 ppm of Span 80. The water volume fraction is 0.5, and the emulsification protocol is the same for all samples. The quantities (in ppm) of Tween 20 added to the water phase of the emulsion are 0, 10, 50, and 160 from left to right, respectively.

curvature of the surfactant film and hence favor coalescence events between water droplets.

We perform a series of bottle tests systematically varying both the concentrations of Span 80 (in oil) and Tween 20 (in water) under the same mixing protocol (Ultra-Turrax 15 000 RPM). We first measure the separated water ratio \mathcal{W}_S as a function of c_0 , the concentration of Span 80 present in the emulsion that we vary while keeping c_D , the concentration of Tween 20, constant. Prior to conducting our experiments, we carefully check that all surfactant mixtures used in our study lead to the formation of W/O emulsions. Figure 3 displays the

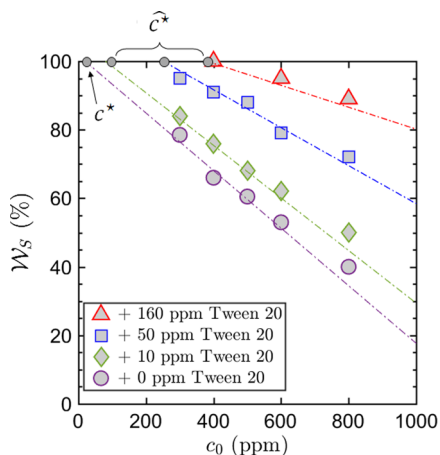


Figure 3. Variation of \mathcal{W}_S with c_0 for four different values of c_D that are reported in the inset. Each experiment is performed thrice, the symbols show the average values, and the error bars are of the order of the symbol size.

variation of \mathcal{W}_S with c_0 for three different values of c_D . To ensure the robustness of our measurements, we perform each bottle experiment thrice. As expected, we observe that for a given value of c_0 , the higher c_D , the larger \mathcal{W}_S . More interestingly, Figure 3 reveals that the variation of \mathcal{W}_S with c_0 still remains linear even if Tween 20 molecules are present in the mixture. Now, if one assumes that the relationship (eq 1) still holds in the presence of Tween 20 molecules, by extrapolating our data with straight lines as shown in Figure 3, one can quantitatively determine how the presence of

Tween 20 affects the value of the minimum concentration of Span 80 required to form the DPL that we next denote by \widehat{c}^* (in the absence of Tween 20 $\widehat{c}^* = c^*$). Compared with the prediction of the model in eq 1, it can be seen from Figure 3 that the presence of Tween 20 molecules in the system increases c^* and reduces the slopes of the linear lines, which correspond to the mean droplet size. In the next paragraph, we develop a theoretical model to rationalize these experimental findings.

THEORETICAL INTERPRETATION

Let us first focus on the variation of \widehat{c}^* with the concentration of Tween 20 added to the system. Qualitatively, the adsorption of Tween 20 molecules at the W/O interface alters the spontaneous curvature of the surfactant film and therefore favors coalescence between water droplets. Since \widehat{c}^* corresponds to the minimum concentration of Span 80 necessary to generate the DPL, it is therefore expected to increase to compensate the competitive adsorption of Tween 20. In the following, we assume that the emulsion stability threshold is set by the surface concentration of the oil-soluble surfactant molecules on the droplet regardless of the concentration of water-soluble surfactant. As later shown, this strong hypothesis is confirmed by the excellent agreement between the data and the model that we herein develop. We rationalize our findings with a simple model, built on the thermodynamic theory of ideal surfactant mixtures. In the sole presence of Span 80 molecules, the Langmuir adsorption isotherm of Span 80 at the water–oil interface reads

$$K_E c_0 = \frac{\Gamma_E}{\Gamma_{\text{sat}}} \frac{1}{1 - \frac{\Gamma_E}{\Gamma_{\text{sat}}}} \quad (2)$$

where K_E and Γ_E are the adsorption coefficient and the surface concentration of Span 80, respectively.

When Tween 20 is added into water at a concentration c_D , Span 80 and Tween 20 molecules now competitively adsorb on the water–oil interface. The isotherm of Span 80 can be deduced from the equation of state for an ideal mixture made of two surfactants,¹⁷ assuming that the molar surfaces of Span 80 and Tween 20 are nearly equal (see the Supporting Information, SI)

$$K_E c_0 = \frac{\widehat{\Gamma}_E}{\Gamma_{\text{sat}}} \frac{1}{1 - \frac{\widehat{\Gamma}_E}{\Gamma_{\text{sat}}} - \frac{\widehat{\Gamma}_D}{\Gamma_{\text{sat}}}} \quad (3)$$

Under this assumption, the surface concentration of Tween 20, $\widehat{\Gamma}_D$, is simply related to that of Span 80, $\widehat{\Gamma}_E$, by:¹⁷ $\widehat{\Gamma}_D = \frac{K_D c_D}{K_E c_0} \widehat{\Gamma}_E$, where K_D is the adsorption coefficient of Tween 20. By substituting this latter relationship into eq 3 and doing some basic algebra, one can straightforwardly obtain

$$\widehat{K}_E c_0 = \frac{\widehat{\Gamma}_E}{\Gamma_{\text{sat}}} \frac{1}{1 - \frac{\widehat{\Gamma}_E}{\Gamma_{\text{sat}}}} \quad (4)$$

where \widehat{K}_E is given by

$$\widehat{K}_E = \frac{K_E}{1 + K_D c_D} \quad (5)$$

Here, \widehat{K}_E corresponds to the adsorption coefficient of Span 80 in the presence of Tween 20. The presence of Tween 20 molecules therefore decreases the adsorption coefficient of Span 80 on the W/O interface. Now, we make the strong assumption that the stability threshold is governed by the surface concentration of the oil-soluble surfactant Span 80, regardless of the surface concentration of Tween 20. We thus keep the same criterion for determining the onset of stability, \widehat{c}^* , as the one used for c^* (when no Tween 20 is present); that is, at a concentration of Span 80 in the bulk such that 80% of the water–oil surface is covered with Span 80, namely, $\Gamma(c^*) = 0.8 \Gamma_{\text{sat}}$ one obtains the following relationship $\widehat{K}_E \widehat{c}^* = K_E c^*$. By using the expression of \widehat{K}_E derived in eq 5, it is then straightforward to derive that

$$\widehat{c}^* \simeq c^*(1 + K_D c_D) \quad (6)$$

Note that this linear relationship, which is derived within the framework of ideal solutions, only holds when c_D is smaller than the critical micelle concentration, c_{CMC} . When $c_D > c_{\text{CMC}}$, the surface tension becomes constant. The chemical potential therefore does no longer vary with surfactant concentration so that one expects that \widehat{c}^* saturates at the value $c^*(1 + K_D c_{\text{CMC}})$.

In Figure 3, we report the values of \widehat{c}^* that we determine for three different values of c_D (10, 50, and 160 ppm). These values of \widehat{c}^* are, respectively, 60, 200, and 400 ppm. From our interfacial tension measurements, we estimate that for Tween 20, $K_D \simeq 0.2 \text{ ppm}^{-1}$ and $c_{\text{CMC}} = 100 \text{ ppm}$ (see the SI). As shown in Figure 4, and although experimental data for only three different concentrations are available, our theoretically predicted values seem to agree well with our experimental data. Note that for $c_D = 160 \text{ ppm}$, the theoretical relationship for \widehat{c}^*

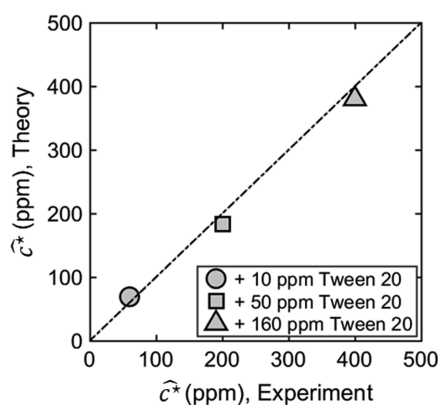


Figure 4. Predicted values of \widehat{c}^* , obtained using eq 6 versus the experimental data. These latter values are extracted by performing systematical bottle test experiments on a model emulsion stabilized by Span 80 to which Tween 20 molecules are added, under the same emulsification protocol. Briefly, the concentration of Span 80 is systematically varied while keeping c_D constant and the water separation ratio, \mathcal{W}_S is measured. The experimental values of \widehat{c}^* are then extracted from these collected data following the procedure described in the legend of Figure 3.

in eq 6 is calculated by replacing c_D by the CMC value, $c_{\text{CMC}} = 100 \text{ ppm}$.

This agreement between experiments and theory confirms our hypothesis that the onset of stability is solely set by the surface coverage of the oil-soluble surfactant regardless of the concentration of the water-soluble surfactant. Therefore, using a thermodynamic theory for describing the competitive adsorption of the two surfactant species at the W/O interface, we are able to derive a quantitative prediction for \widehat{c}^* (the minimum concentration of Span 80 in solution necessary to obtain a DPL, when Tween 20 is added to the system), in terms of the parameters at play in the problem, as shown in eq 6.

By replacing c^* by \widehat{c}^* in eq 1, and using eq 6, one obtains a theoretical relationship yielding the water separation efficiency \mathcal{W}_S , as a function of c_D , the concentration of the demulsifier added to the system, as shown below

$$\mathcal{W}_S \simeq 1 - \frac{R_0}{3\Gamma_{\text{sat}}} \frac{1 - \Phi}{\Phi} [c_0 - c^*(1 + K_D c_D)] \quad (7)$$

Our simple model shown in eq 7 demonstrates that the increase of water separation efficiency \mathcal{W}_S , observed when a demulsifier is added to an emulsion system, is strongly correlated to the adsorption strength K_D of the demulsifier molecules onto the W/O interface. The adsorption of the demulsifier molecules enters into competition with that of the emulsifier molecules and therefore leads to a significant increase of the critical concentration of emulsifiers, \widehat{c}^* , required to generate the DPL, and consequently, also to higher \mathcal{W}_S . Equation 7 predicts that if the concentration of demulsifier, c_D , is varied while keeping all other experimental conditions fixed, then the water separation efficiency \mathcal{W}_S should linearly increase with c_D as depicted in Figure 5.

However, when the demulsifier is introduced into the aqueous phase prior to emulsification, there exists another additional effect that must be considered for well describing the variation of \mathcal{W}_S with c_D . This effect is indeed related to the variation with c_D of R_0 , the mean droplet size formed after emulsification. By lowering the W/O interfacial tension of the system, the presence of Tween 20 (the demulsifier) leads to the formation of smaller droplets during emulsification (see the SI). Since at high Reynolds numbers, the mean droplet size results from a balance between the droplet interfacial and inertial stresses,¹⁸ R_0 scales—for a given Reynolds number—as $\gamma^{3/5}$, where γ is the W/O interfacial tension of the system, as experimentally reported.¹⁹ If one considers that R_0 varies with γ , according to this scaling law, it is then straightforward to establish from eq 7 that: $(1 - \mathcal{W}_S) \sim \gamma^{3/5}(c_0 - \widehat{c}^*)$. As shown in Figure 6, this prediction is in very good agreement with our experimental observations.

APPLICATION TO WATER-IN-CRUDE OIL EMULSIONS

By working with a W/O emulsion model system stabilized by Span 80, we have previously investigated the effect of adding a water-soluble surfactant (Tween 20) that acts as a demulsifier on the formation and thickness of the DPL layer. We have shown that adding even a small amount of Tween 20 may significantly reduce the thickness of the DPL and henceforth increases \mathcal{W}_S , the fraction of demixed water that is retrieved

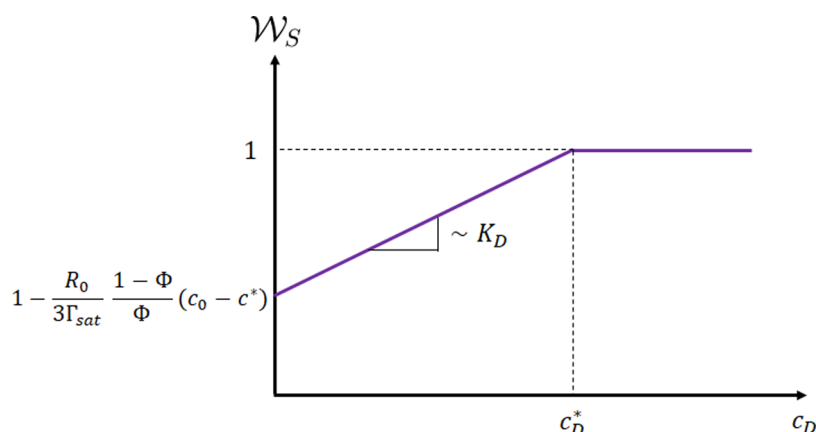


Figure 5. Plot showing the theoretically predicted variation of \mathcal{W}_S with c_D , the concentration of demulsifier added to the emulsion. Herein, we assume that $c_D^* \leq c_{CMC}$.

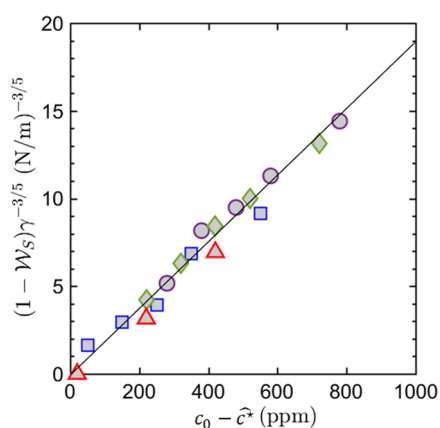


Figure 6. $(1 - \mathcal{W}_S)\gamma^{-3/5}$ versus $(c_0 - \hat{c}^*)$ found for four emulsions systems having different concentrations of Tween 20 as indicated in the inset and emulsified under the same operating mechanical conditions (i.e., same Reynolds number). The W/O interfacial tensions that are measured for these various emulsion systems do not depend on c_0 , the concentration of Span 80, provided that $c_0 > 100$ ppm. The values obtained for γ (in mN/m) are 5.2, 4.1, 3.2, and 0.8 for $c_D = 0, 10, 50,$ and 160 ppm, respectively (see the SI).

when the DPL forms. We have developed a simple model built on the thermodynamics of ideal solutions that very well describes the variation of \mathcal{W}_S with the experimental parameters, characterizing the emulsion. Our main objective is now to determine whether the prediction made by this theoretical model, and hence the assumption that the surface coverage of the oil-soluble surfactant that governs the onset of coalescence remains the same regardless of the concentration of the water-soluble surfactant, and the assumption that an ideal analysis of the surface thermodynamics are still valid in the case of water-in-crude oil emulsion systems. The latter, generally based on Langmuir isotherms, has already been applied to systems containing asphaltenes.^{20,21} To answer this question, we have taken a close look at the scientific literature, in search for experimental reports in which the authors have studied the effect of chemical demulsifiers on the stability of crude oil emulsions varying systematically the concentration of added demulsifier while reporting the corresponding values of the W/O interfacial tensions.

The first paper found, which complies with these specifications, concerns the work of Kedar et al.⁷ In that

article, the authors compare the emulsion separation efficiency of various additives at different chemical dosages. In good agreement with our bottle test observations, they also report the existence of a fast kinetic regime before a DPL layer forms, separating water and oil demixed phases. To characterize the efficiency of the demulsifiers, they determine what they call the water separation efficiency, that is, the amount of water that has demixed when the DPL forms. This variable is in total adequation to what we name \mathcal{W}_S . Very interestingly, when we plot their measured water separation efficiencies, \mathcal{W}_S , as a function of the additive concentrations, we observe that all data fall in straight lines (Figure 7). This experimental finding very well confirms the prediction made by our theoretical model (see eq 7) that claims that \mathcal{W}_S linearly increases with c_D , the concentration of the demulsifier agent. Since the slope of this straight line is proportional to K_D , the adsorption coefficient of the demulsifier on the W/O interface, and the

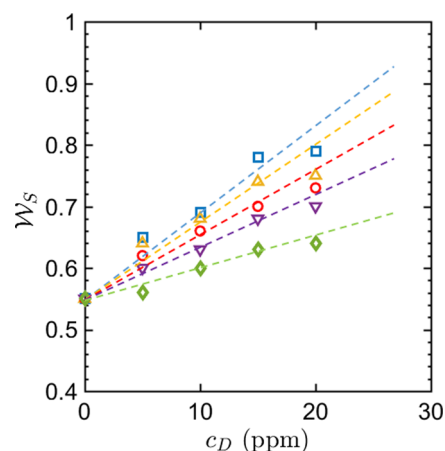


Figure 7. Data reproduced from Kedar et al.⁷ Variations of \mathcal{W}_S with c_D observed for five different surfactant demulsifiers added to the system. These demulsifiers, which have the same hydrophobic chain but different head groups, are, respectively, sodium lauryl ether sulfate (SLES) (blue square), sodium lauryl sulfate (SLS) (orange triangle), benzalkonium chloride (BKC) (red circle), polyoxyethylene 23 lauryl ether ($C_{12}E_{23}$) (violet triangle down), and lauryl alcohol ethoxylate 7 mole ($C_{12}E_7$) (green diamond). As reported by Kedar et al.,⁷ all W/O emulsions are prepared by mixing deionized water with crude oil provided by ONGC Uran Pvt Ltd under similar mixing conditions.

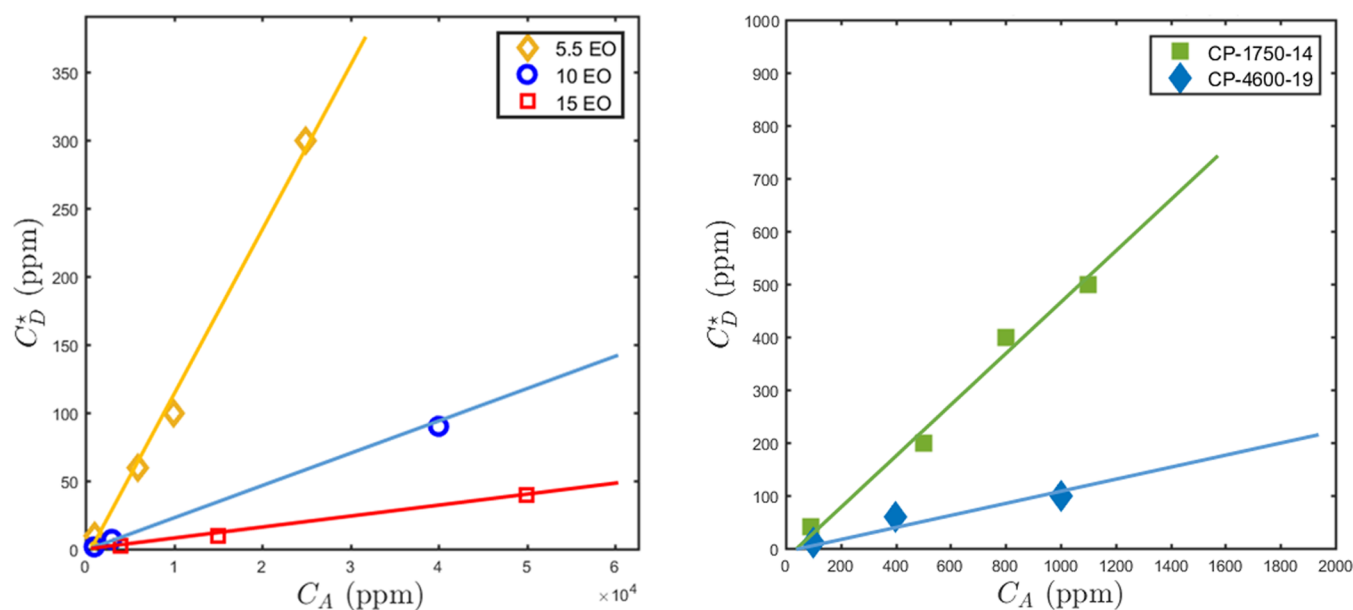


Figure 8. (Left) Data reproduced from Rondón et al.⁹ displaying the ethoxylated nonylphenol demulsifier concentrations for optimal formulation (c_D^*) that are determined as a function of the asphaltene concentration, c_A , for three different values EO of average ethylene oxide number (EON): 5,5 (orange diamond), 10 (blue circle), and 15 (red square). The W/O emulsions are prepared by mixing an aqueous phase containing the demulsifier and Vic-Bill crude oil diluted in cyclohexane under the same operating protocol and the constant volume fraction of oil. (Right) Data reproduced from Pereira et al.¹⁰ showing c_D^* determined as a function of c_A when two different demulsifiers CP-1750-14 (green solid square) and CP-4600-19 (blue solid diamond) (two triblock copolymers) are added to a water-in-crude oil emulsion. This emulsion is obtained by emulsifying 5 mL of the aqueous phase containing the demulsifier and 5 mL of a crude oil diluted with cyclohexane so that the asphaltene concentration is c_A . All emulsions are prepared under the same mixing conditions.

stronger is K_D , the higher the efficiency water separation must be.

Other studies that have attracted our interest are the works of Rondón et al.,⁹ Borges et al.,¹¹ and Pereira et al.¹⁰ that deal with the breaking of water-in-crude oil emulsions. In these studies, the authors investigate the stability of crude oil emulsions in the presence of demulsifier additives. They systematically vary the asphaltene concentration known to stabilize water-in-crude oil emulsions by diluting crude oil in oily solutions. They report a linear relationship between the additive concentration c_D^* at minimum stability and c_A , the asphaltene concentration that is witnessed only when c_A is smaller than a threshold value. As discussed below, this experimental observation can also be well explained by our theoretical model. To start, we first note that since the presence of additive surfactant increases the water separation efficiency \mathcal{W}_S , the minimum stability of the emulsion occurs when \mathcal{W}_S reaches a value close to 1. Therefore, we next assume that for c_D^* , $1 - \mathcal{W}_S = \epsilon \simeq 1\%$. As asphaltene species are well known to act as stabilizers for W/O crude oil emulsion systems, we reasonably consider that c_A indeed corresponds to the variable, c_θ , previously defined in our model. Using eq 7 and the previous criterion established for the definition of c_D^* , it is then straightforward to demonstrate the existence of a linear relationship between c_D^* and c_A

$$c_D^* \simeq \frac{1}{c^* K_D} c_A - \frac{1}{K_D} - \epsilon \frac{3\Gamma_{\text{sat}}}{c^* K_D R_0} \frac{\Phi}{1 - \Phi} \quad (8)$$

As derived in eq 8, the slope of c_D^* versus c_A depends on the inverse of the adsorption coefficient, K_D , of the demulsifier additives on the W/O interface. Hence, the larger the adsorption strength of the additives is, the more efficient is their destabilization of the emulsion, and consequently smaller

is c_D^* . These predictions very well concur with the experimental findings reported by Pereira et al. and Rondón et al. as depicted in Figure 8.

Furthermore, in another work,¹¹ the authors investigate the effects of the water–oil ratio over both c_D^* and the validity of the linear relationship, previously reported between c_D^* and c_A . They experimentally observe that this linear relationship remains valid even when the water–oil ratio is varied; however, they find that the value of c_D^* decreases as, Φ , the volume fraction of water in the system increases. As shown in Figure 9, these additional experimental results very well agree with the predictions of our model (see eq 8) that anticipates for a fixed value of c_A , a linear variation of c_D^* with $\Phi/(1 - \Phi)$. By plotting the values of c_D^* measured by Borges et al.¹¹ for different values of c_A , as a function of $\Phi/(1 - \Phi)$, we observe that the intersections of the respective linear fits with the y-axis well correspond with the values of c_A , as predicted by our model.

Surprisingly, and despite its simplicity, the observations done on a model system have proved to be also valid on various crude oil/water emulsion, highlighting the generality of our approach.

CONCLUSIONS

To conclude, we have shown that the efficiency of a demulsifier for destabilizing a W/O emulsion strongly correlates with its adsorption strength at the water–oil interface. More precisely, the adsorption of the emulsifier appears to be the only factor responsible for the onset of stability against coalescence. Because its adsorption competes with that of the demulsifier, the presence of the demulsifier leads to a smaller dense packed layer (DPL). By combining the theoretical approach recently introduced by Dinh et al.¹⁵ to describe the destabilization

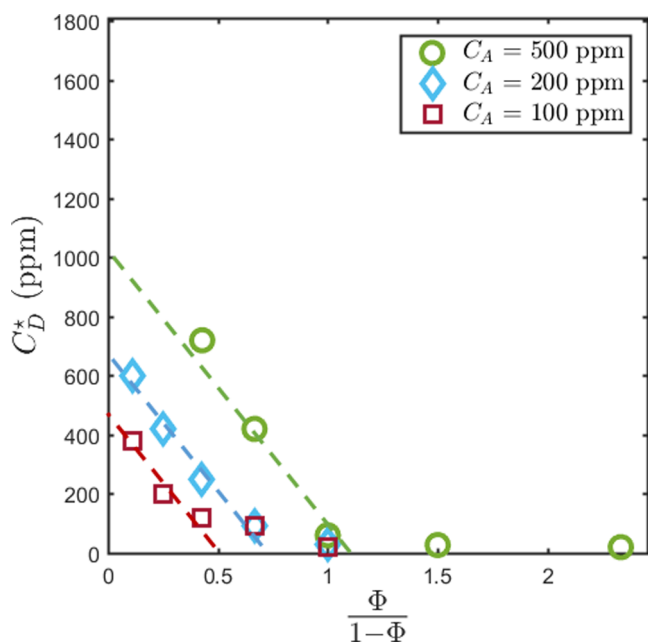


Figure 9. Data reproduced from Borges et al.¹¹ showing c_D^* plotted as a function of $\Phi/(1 - \Phi)$ for three different values (given in ppm) of c_A : 500 (green circle), 200 (blue diamond), and 100 (red square). The W/O emulsion system consists of an aqueous phase containing an ethoxylated iso-tridecanol, commercialized as GENAPOL X-159 by Clariant, which acts as a demulsifier, and an oil phase, which consists of crude oil (from San Jacinto field in Peru) diluted in cyclohexane. All emulsions are generated under the same operating conditions.

kinetics of W/O emulsions occurring in bottle test experiments and the thermodynamics of ideal solutions, we have built a simple model that very well portrays the occurrence and thickness of the DPL when a demulsifier is added to the system. We have established an analytical formula that predicts for bottle tests the water separation efficiency, \mathcal{W}_s , a function of the key parameters of the problem, namely, the water volume fraction, the mean droplet size, the concentration of both the emulsifier and the demulsifier added to the aqueous phase, and the adsorption coefficient of the demulsifier. Our theoretical results show that the concentration of the demulsifier for optimal formulation is expected to vary both linearly with that of the emulsifier and with the inverse of the adsorption coefficient of the demulsifier at the water–oil interface. These predictions very well concur with experimental observations reported in the scientific literature on a wide range of water-in-crude oil emulsion systems, which shows the value of our approach for the petroleum industry. Our simple analytical model could serve as a guidance to select the demulsifiers in emulsion science since our theoretical framework should work on both W/O and O/W emulsion systems.

MATERIALS AND METHODS

Emulsion Preparation and Bottle Tests. The continuous oil phase used for our model emulsion systems is *n*-dodecane (99% pure) (Acros Organics ref 117590025) to which we add varying concentrations of Span 80 (Fisher Scientific; ref 15474919), a surfactant known to naturally promote the formation of water-in-oil emulsions. We add 10 mM sodium chloride (Fisher Scientific) to ultrapure Milli-Q water (resistivity, 18 M Ω ·cm) to first screen out all possible

electrostatic interactions resulting from residual traces of ionic surfactants²² and second to prevent Ostwald ripening from being the prevalent destabilization mechanism. To investigate the effect of a demulsifier additive on this emulsion, we add Tween 20, a water-soluble surfactant, known to naturally promote the formation of O/W emulsions. All our bottle tests presented herein after are performed in 24 mL cylindrical vials having a constant diameter of approximately 2 cm and a constant temperature of 23 °C. The water/oil volume ratio is set to 1:1, and the total volume of fluids is set to 15 mL. We proceed as follows: we first pour 7.5 mL of water (with or without Tween 20) into the vial that we next complete with an additional volume of 7.5 mL of oil (containing Span 80). Since water and dodecane are partially miscible, we let both fluids equilibrate at rest for 30 min before mechanically emulsifying the system. Emulsions are produced by mixing the two phases using an Ultra-Turrax (IKA-T10, from IKA) operating at 15 000 rpm.

We next quantify the emulsion stability by following the kinetics of the interface between the demixed water phase and the DPL as depicted in Figure 1. The position of this interface, which is measured from the bottom of the vial, is denoted by H_w . To capture H_w at different stages of the destabilization process, we image the vial at regularly time-spaced intervals with a Nikon DS100 camera using backlighting. For each snapshot, we extract H_w , the position of water/emulsion interface, using a custom-written MATLAB image processing software. As this interface is not a horizontal straight line notably because of the presence of a meniscus, we determine H_w as follows. We average the intensity of the image about the *x*-direction and observe the intensity profile of this average along the vertical *z*-direction of the vial height. Taking the derivative of this averaged intensity profile then allows one to readily extract the positions of the two interfaces. As illustrated in Figure 1, the emulsion destabilization kinetics is determined by the time evolution of the water separation ratio \mathcal{W} , defined as the ratio of the volume of demixed water to the total volume of water present in the system

$$\mathcal{W} = \frac{H_w}{H_0} \quad (9)$$

where H_0 is the height of the water column in the vial prior to emulsification.

Interfacial Tension Measurements. The nature (O/W or W/O) of an emulsion greatly depends on the type and amounts of surfactant molecules that it contains. By modifying the W/O interfacial tension, these parameters also play a key role in the selection of the droplet size under mechanical stirring and in the stability of the final emulsion. When systematically studying emulsion systems, this requires to well characterize the variation of the W/O interfacial tension with the concentration of surfactant. We measure the W/O interfacial tension of our model W/O emulsion using a commercial pendant drop tensiometer (Tracker, from TECLIS-Scientific, France). With this classical pendant drop method, the W/O surface tension is calculated from the shadow image of a 20 μ L pendant water drop immersed in the bulk dodecane oil using shape analysis at a temperature of 23 °C. The water drop forms at the tip of a calibrated needle having an inner diameter of 2 mm. Note that prior to our measurements, we carefully let water and oil phases be in contact for at least 24 h to ensure that the equilibrium partition

of the surfactant molecules between both phases is achieved. By systematically varying the concentration of Span 80 and Tween 20 that are solubilized in oil and water, respectively, we can extract their isotherm adsorption curves (see the SI).

■ ASSOCIATED CONTENT

SI Supporting Information

The Supporting Information is available free of charge at <https://pubs.acs.org/doi/10.1021/acsomega.1c03848>.

Measurement of IFT as a function of Span 80 and Tween 20 concentrations; dynamic IFT measurements for mixtures of Span 80 and Tween 20; and distribution of droplets size through microscopy measurement for the cases with and without Tween 20 (PDF)

■ AUTHOR INFORMATION

Corresponding Authors

Huy-Hong-Quan Dinh – *Laboratoire Physico-Chimie des Interfaces Complexes, Bâtiment CHEMSTARTUP, 64170 Lacq, France; TOTAL S.A., Pôle d'Etudes et de Recherches de Lacq, 64170 Lacq, France; orcid.org/0000-0002-2353-3219; Email: huy-hong-quan@totalenergies.com*

Pascal Panizza – *Laboratoire Sciences et Ingénierie de la Matière Molle, ESPCI Paris, PSL University, Sorbonne Université, CNRS UMR 7615, F-75005 Paris, France; IPR, UMR CNRS 6251, Campus Beaulieu, Université Rennes 1, 35042 Rennes, France; orcid.org/0000-0003-4738-733X; Email: pascal.panizza@univ-rennes1.fr*

Authors

Enric Santanach-Carreras – *Laboratoire Physico-Chimie des Interfaces Complexes, Bâtiment CHEMSTARTUP, 64170 Lacq, France; TOTAL S.A., Pôle d'Etudes et de Recherches de Lacq, 64170 Lacq, France*

Véronique Schmitt – *Centre de Recherche Paul Pascal, 33600 Pessac, France; orcid.org/0000-0002-9938-9911*

François Lequeux – *Laboratoire Sciences et Ingénierie de la Matière Molle, ESPCI Paris, PSL University, Sorbonne Université, CNRS UMR 7615, F-75005 Paris, France; orcid.org/0000-0003-4076-3988*

Complete contact information is available at:

<https://pubs.acs.org/doi/10.1021/acsomega.1c03848>

Notes

The authors declare no competing financial interest.

■ ACKNOWLEDGMENTS

This work was funded by a French CIFRE Fellowship (contract number 2018-0911) with TotalEnergies S.A. The authors acknowledge TotalEnergies S.A. management for giving them permission to publish their results. They thank Maurice Bourrel, Nicolas Passade-Boupat, and Thierry Palermo for many fruitful discussions. They also thank Didier Lauranson for his support in their daily lab activities.

■ REFERENCES

- (1) Pal, R. Techniques for measuring the composition (oil and water content) of emulsions—A state of the art review. *Colloids Surf., A* **1994**, *84*, 141–193.
- (2) Frising, T.; Noik, C.; Dalmazzone, C. The Liquid/Liquid Sedimentation Process: From Droplet Coalescence to Technologically Enhanced Water/Oil Emulsion Gravity Separators: A Review. *J. Dispersion Sci. Technol.* **2007**, *27*, 1035–1057.

- (3) Schramm, L. L. Petroleum Emulsions. In *Emulsions: Fundamentals and Applications in the Petroleum Industry*; Schramm, L. L., Eds.; Advances in Chemistry Series 231; American Chemical Society, 1992; pp 1–49.

- (4) Kilpatrick, P. K.; Spiecker, P. M. Asphaltenes Emulsions. In *Encyclopaedic Handbook of Emulsion Technology*, 1st ed.; Sjoblom, J., Ed.; CRC Press, 2001; pp 707–730.

- (5) Rondón, M.; Bouriat, P.; Lachaise, J.; Salager, J.-L. Breaking of Water-in-Crude Oil Emulsions. 1. Physicochemical Phenomenology of Demulsifier Action. *Energy Fuels* **2006**, *20*, 1600–1604.

- (6) Goldszal, A.; Bourrel, M. Demulsification of Crude Oil Emulsions: Correlation to Microemulsion Phase Behavior. *Ind. Eng. Chem. Res* **2000**, *39*, 2746–2751.

- (7) Kedar, V.; Bhagwat, S. S. Effect of polar head surfactants on the demulsification of crude oil. *Pet. Sci. Technol.* **2018**, *36*, 91–98.

- (8) Razi, M.; Rahimpour, M. R.; Jahanmiri, A.; Azad, F. Effect of a Different Formulation of Demulsifiers on the Efficiency of Chemical Demulsification of Heavy Crude Oil. *J. Chem. Eng. Data* **2011**, *56*, 2936–2945.

- (9) Rondón, M.; Pereira, J. C.; Bouriat, P.; Graciaa, A.; Lachaise, J.; Salager, J.-L. Breaking of Water-in-Crude-Oil Emulsions. 2. Influence of Asphaltene Concentration and Diluent Nature on Demulsifier. *Energy Fuels* **2008**, *22*, 702–707.

- (10) Pereira, J. C.; Delgado-Linares, J.; Scorzza, C.; Rondon, M.; Rodríguez, S.; Salager, J.-L. Breaking of Water-in-Crude Oil Emulsions. 4. Estimation of the Demulsifier Surfactant Performance To Destabilize the Asphaltenes Effect. *Energy Fuels* **2011**, *25*, 1045–1050.

- (11) Borges, B.; Rondon, M.; Sereno, O.; Asuaje, J. Breaking of Water-in-Crude-Oil Emulsions. 3. Influence of Salinity and Water-Oil Ratio on Demulsifier Action. *Energy Fuels* **2009**, *23*, 1568–1574.

- (12) Le Follotec, A. L.; Pezron, I.; Noik, C.; Dalmazzone, C.; Metlas-Komunjera, L. Triblock copolymers as destabilizers of water-in-crude oil emulsions. *Colloids Surf., A* **2010**, *365*, 162–170.

- (13) Noik, C.; Palermo, T.; Dalmazzone, C. Modeling of Liquid/Liquid Phase Separation: Application to Petroleum Emulsions. *J. Dispersion Sci. Technol.* **2013**, *34*, 1029–1042.

- (14) van Aken, G. A.; Zoet, F. D. Coalescence in Highly Concentrated Coarse Emulsions. *Langmuir* **2000**, *16*, 7131–7138.

- (15) Dinh, H.-H.-Q.; Santanach-Carreras, E.; Schmitt, V.; Lequeux, F. Coalescence in concentrated emulsions: Theoretical predictions and comparison with experimental bottle test behaviour. *Soft Matter* **2020**, *16*, 10301–10309.

- (16) Riechers, B.; Maes, F.; Akoury, E.; Semin, B.; Gruner, P.; Baret, J.-C. Surfactant adsorption kinetics in microfluidics. *Proc. Natl. Acad. Sci. U.S.A.* **2016**, *113*, 11465–11470.

- (17) Lucassen-Reynders, E. Competitive adsorption of emulsifiers 1. Theory for adsorption of small and large molecules. *Colloids Surf., A* **1994**, *91*, 79–88.

- (18) Boxall, J. A.; Koh, C. A.; Sloan, E. D.; Sum, A. K.; Wu, D. T. Droplet Size Scaling of Water-in-Oil Emulsions under Turbulent Flow. *Langmuir* **2012**, *28*, 104–110.

- (19) Arinina, M. P.; Zuev, K. V.; Kulichikhin, V. G.; Malkin, A. Y. Effect of Composition and Interfacial Tension on the Rheology and Morphology of Heavy Oil-In-Water Emulsions. *ACS Omega* **2020**, *5*, 16460–16469.

- (20) Morais, W. J. S.; Franceschi, E.; Dariva, C.; Borges, G. R.; Santos, A. F.; Santana, C. C. Dilatational Rheological Properties of Asphaltenes in Oil–Water Interfaces: Langmuir Isotherm and Influence of Time, Concentration, and Heptol Ratios. *Energy Fuels* **2017**, *31*, 10233–10244.

- (21) Mohammadi, M.; Zirrahi, M.; Hassanzadeh, H. Adsorption Kinetics of Asphaltenes at the Heptol–Water Interface. *Energy Fuels* **2020**, *34*, 3144–3152.

- (22) Roger, K.; Cabane, B. Why Are Hydrophobic/Water Interfaces Negatively Charged. *Angew. Chem., Int. Ed.* **2012**, *51*, 5625–5628.